A BLIND EQUALIZATION ALGORITHM FOR MULTIMODULUS SQUARE-QAM SIGNALS

Shafayat Abrar and Asoke Kumar Nandi

Dept. of Electrical Engineering and Electronics
The University of Liverpool, Liverpool L69 3GJ, UK
email: {shafayat,aknandi}@liverpool.ac.uk

ABSTRACT

We present a generic and an efficient multimodulus family of blind equalization algorithm for use in the higher-order quadrature amplitude modulation based digital communication systems. The proposed algorithm is memoryless Bussgang-type and is based on a stochastic gradient descent of a constrained convex cost function. We show it to be capable of blindly equalizing the channel and recovering the carrier phase simultaneously. We also provide the dynamic convergence analysis of the proposed adaptive algorithm.

1. INTRODUCTION

We consider a baseband linear time-invariant single-input-single-output discrete-time system. We assume that the transmitted sequence $\{a_n\}$ is independently and identically-distributed (i.i.d.), and takes values of square-quadrature amplitude modulation (QAM) symbols $\mathscr{A}$. The received signal is expressed as: $x_n = \mathbf{h}^T \mathbf{a}_n + \vartheta_n$, where $\mathbf{a}_n$ is data vector, $\mathbf{h}$ is the impulse response (vector) of symbol-rate moving-average channel, and ϑ_n is additive white Gaussian noise. The output of N-tap equalizer is: $y_n = \mathbf{w}_n^H \mathbf{x}_n$, where $\mathbf{w}_n = [w_{n,0}, \cdots, w_{n,N-1}]^T$ is the vector of equalizer's coefficients and $\mathbf{x}_n = [x_n, \cdots, x_{n-N+1}]^T$ is the channel observation vector; the superscripts ^{T} and ^{H} denote transpose and conjugate-transpose, respectively.

The idea behind the *Bussgang* blind equalization (BE) algorithm is to minimize (or maximize), through the choice of the equalizer filter coefficients $\mathbf{w}$, a certain cost-function depending on the equalizer output y_n such that y_n provides an estimate of the source signal $a_n \in \mathscr{A}$ up to some inherent indeterminacies, $y_n = \alpha a_{n'}, n' = n - \tau$ with $\alpha = |\alpha| e^{\imath\gamma} \in \mathbb{C}$, $\tau \in \mathbb{Z}$ where $|\alpha|$ and τ represent an arbitrary gain and delay, respectively. The phase γ represents an isomorphic rotation of the symbol constellation. A Bussgang BE algorithm tries to solve the following problem:

$$\mathbf{w} = \arg\min_{\mathbf{w}} J, \text{ with } J = \mathbb{E}[\mathscr{J}(y_n)] \tag{1}$$

where the cost J is an expression for higher-order statistics of y_n and $\mathscr{J}(y_n)$ is a real-valued function. The equalization is accomplished when equalized sequence y_n acquires an identical distribution as that of the channel input a_n [1]. If the *minimization* is realized by stochastic gradient-based adaptive method, then the updating rule is

$$\mathbf{w}_{n+1} = \mathbf{w}_n - \mu \left(\frac{\partial \mathscr{J}}{\partial \mathbf{w}_n}\right)^* = \mathbf{w}_n + \mu \Phi(y_n)^* \mathbf{x}_n, \quad \text{with } \Phi(y_n) \equiv -\frac{\partial \mathscr{J}}{\partial y_n^*}. \tag{2}$$

where $\mu > 0$ is a small positive adaptation step-size.[1] The complex-valued *error-function* $\Phi(y_n)$ can be understood as an estimate of the difference between the desired and the actual equalizer outputs.

Existing gradient descent-based Bussgang BE algorithms differ mainly by the particular cost function used. They all adopt non-convex cost functions that can become multimodal for finite equalizer parameterizations and hence do not preclude the possibility of a non-open eye solution. Contrariwise, gradient descent of convex cost functions implies unimodal convergence and therefore avoids the local minima problem [2]. The second major issue is to resolve the phase ambiguity. Ideally the adaptation scheme should provide both equalization (removal of intersymbol interference (ISI) except for a gain factor) and carrier phase-recovery (to rotate the output constellation to the correct orientation before quantization) simultaneously.

In this paper, we study a family of memoryless BE algorithms that is based on the stochastic gradient descent adaptive optimization of a constrained and approximated convex cost-function. In Section 2, we introduce the cost-function and resulting algorithm. In Section 3, we provide the dynamic convergence expressions of the proposed algorithm. In Sections 4 and 5, we provide, respectively, computer simulations and conclusions. In the sequel, we will use notations $\Re[\cdot]$ (or subscript R) and $\Im[\cdot]$ (or subscript I) to represent the real- and imaginary-parts of the enclosed complex entity, respectively. A subscript L will be used to denote either R or I.

2. PROPOSED ALGORITHM

The cost-function based Bussgang BE algorithms have been studied to be *non-convex* in nature [12]. The non-convexity may lead to undesirable local minima resulting in insufficient removal of channel distortion [2]. A convex cost-function which has been specifically designed for square-QAM is that of Kennedy and Ding [4], which suggested to minimize the following:

$$\max\left\{\left|y_{R,n}\right|\right\} + \max\left\{\left|y_{I,n}\right|\right\} = \|\{y_{R,n}\}\|_\infty + \|\{y_{I,n}\}\|_\infty \tag{3}$$

The convexity of cost (3) with respect to the equalizer coefficient vector $\mathbf{w}$ follows from the triangle inequality under the assumption that all input sequences are possible. The cost (3) was minimized under a linear constraint $\Re[w_{n,\kappa}] + \Im[w_{n,\kappa}] =$

[1] Expression (2) exploits the fact that (for $\mathscr{J} \in \mathbb{R}$ and $y_n = \mathbf{w}_n^H \mathbf{x}_n$):

$$\left(\frac{\partial \mathscr{J}}{\partial \mathbf{w}}\right)^* = \left(\frac{\partial \mathscr{J}}{\partial y_n^*}\frac{\partial y_n^*}{\partial \mathbf{w}}\right)^* = \left(\frac{\partial \mathscr{J}}{\partial y_n^*}\frac{\partial \mathbf{x}_n^H \mathbf{w}}{\partial \mathbf{w}}\right)^* = -\Phi(y_n)^* \mathbf{x}_n.$$

 ISSN 2076-1465

1, where $w_{n,\kappa}$ is the anchored tap at κth position (to avoid all-zero situation). Due to the linearity of this constraint, the convexity of (3) with respect to both the real and imaginary parts of the equalizer coefficients is maintained, and global convergence is therefore assured. However, (3) cannot be exactly evaluated in practice with finite data length, the following approximation was used:

$$\min_{\mathbf{w}} \left\{ \mathbb{E}\left[|y_{R,n}|^{p+2} \right] + \mathbb{E}\left[|y_{I,n}|^{p+2} \right] \right\}, \tag{4a}$$

$$\text{s.t. } \Re[w_{n,\kappa}] + \Im[w_{n,\kappa}] = 1, \quad (\text{large } p) \tag{4b}$$

Expression (4a) is based on the fact that, given a large p', the global minimum of the $l_{p'}$ norm will be close to the global minima of the l_∞ norm. Using a polar representation, [4] suggested to adapt $w_{n,\kappa}$ as follows:

$$\varpi_{n+1} = \varpi_n + \mu_2 \frac{\left(|y_{R,n}|^p y_{R,n} c_R + |y_{I,n}|^p y_{I,n} c_I\right)}{\left(\cos\varpi_{n+1} + \sin\varpi_{n+1}\right)^2} \tag{5a}$$

$$w_{n+1,\kappa} = \frac{\exp\left(\imath\varpi_{n+1}\right)}{\cos\varpi_{n+1} + \sin\varpi_{n+1}}, \tag{5b}$$

where $(-\pi/4 < \varpi_n < 3\pi/4)$, $c_R = \Re[x_{n-\kappa}] - \Im[x_{n-\kappa}]$ and $c_I = \Re[x_{n-\kappa}] + \Im[x_{n-\kappa}]$. For $0 \le (i \ne \kappa) \le N-1$, *viz*

$$w_{n+1,i} = w_{n,i} - \mu_1 \left[|y_{R,n}|^p y_{R,n} - \imath |y_{I,n}|^p y_{I,n} \right] x_{n-i} \tag{6}$$

where $\imath \doteq \sqrt{-1}$ and $\mu_1, \mu_2 > 0$. We refer to (5)-(6) as Kennedy-Ding algorithm (KDA). We found that, for 4/16-QAM, the performance of KDA is largely improved if larger p is selected. However, the residual ISI floor achieved by KDA is either similar to or mostly much inferior to those obtained from non-convex Bussgang BE algorithms, like the conventional constant modulus algorithm (CMA) [5] and/or multimodulus algorithm (MMA) [6]. For higher-order QAM ($\ge$ 64-QAM), the eye-opening is either achieved only by allowing a very slow convergence or not achieved at all. So, in spite of its global convergence behavior, its application is found to be quite limited to small constellations.

We note that the tap-anchoring constraint (4b) can be adjusted within the cost-function (4a) leading to the relaxation of the requirements of separate tap-anchoring and automatic gain control. A possible constrained solution is

$$J = \mathbb{E}\left[|y_{R,n}|^{p+2} + |y_{I,n}|^{p+2} \right] + \lambda \left(\mathbb{E}\left[|y_n|^2 \right] - P_a \right) \tag{7}$$

where λ is Lagrangian multiplier and $P_a = \mathbb{E}\left[|a_n|^2 \right]$, so the equalizer average output energy is constrained to be equal to that of the transmitted signal. The stochastic gradient-descent realization gives the following update:

$$\mathbf{w}_{n+1} = \mathbf{w}_n + \mu \left[\left(R_R^p - |y_{R,n}|^p \right) y_{R,n} - \imath \left(R_I^p - |y_{I,n}|^p \right) y_{I,n} \right] \mathbf{x}_n \tag{8}$$

where $R_L^p = -2\lambda/(p+2)$ is a constant. We denote (8) as *pth-order constrained multimodulus algorithm*, cMMA(p). The term multimodulus was used because of its significant similarity with the multimodulus algorithm reported in [6].

It is easy to show that (due to the constraint), cMMA(p) does not require separate tap-anchoring and/or additional AGC for true energy conservation, provided the constant R_L^p (or equivalently λ) is correctly evaluated. Notice that cMMA(p) generalizes a number of existing algorithms. Like, for $p = 1$ and 2, it becomes equivalent to the algorithms appeared in [7] and [6], respectively.

2.1 Evaluation of Dispersion Constant

Here we discuss the evaluation of Lagrange multiplier λ in (7). Since $R_L^p = -2\lambda/(p+2)$, we can equivalently focus on the evaluation of dispersion constants R_L. The dispersion constant is considered as the *statistical gain* of equalizer and it contains *embedded* information about the true energy of the transmitted signal. According to Bellini [1], *the (dispersion) constant, which controls the equalizer amplification, is chosen to give zero tap-gain increments when perfect equalization is achieved*, i.e., $\mathbb{E}[\Phi(y_n)^* x_{n-i}] = 0$.

Upon convergence, we can assume $y_n = a_{n-\tau} + u_n$, where u_n constitutes the sum of additive noise (ϑ_n) through the filter and it is zero-mean Gaussian; u_n is known as *convolutional noise*. Ignoring the small correlation between y_n and additive noise ϑ_{n-i}, we get $\mathbb{E}\left[\Phi(a_{n-\tau} + u_n)^* \sum_{j=0}^{K-1} h_j a_{n-j-i} \right] = 0$. We notice that the expected values in the sum are zero whenever $n - \tau \ne n - j - i$; on the other hand, considering channel coefficients constant, we get $\mathbb{E}[\Phi(a_{n-\tau} + u_n)^* a_{n-\tau}] = 0$. Since in cMMA($p$), the $\Phi(\cdot)$ is a decoupled function of i.i.d. quadrature components, we only need to solve for one of the quadrature components. So the evaluation of R_L requires the solution of $\mathbb{E}\left[a_L (a_L + v) \left(|a_L + v|^p - R_L^p \right) \right] = 0$, where we use v to denote either the in-phase or quadrature component of u_n and its variance is σ_v^2. For $p = 1$, we obtain

$$R_L = \frac{\mathbb{E}\left[2a_L (a_L^2 + \sigma_v^2) Q\left(-\frac{a_L}{\sigma_v} \right) + \sqrt{\frac{2}{\pi}} a_L^2 \sigma_v \exp\left(-\frac{a_L^2}{2\sigma_v^2} \right) \right]}{\mathbb{E}\left[a_L^2 \right]} \tag{9}$$

Under the limit, σ_v tends to zero, (9) simplifies to the value that appeared in [7], i.e., $R_L = \mathbb{E}\left[|a_L|^3 \right] / \mathbb{E}\left[a_L^2 \right]$. For $p = 2$, we obtain

$$R_L^2 = 3\sigma_v^2 + \left(\mathbb{E}\left[a_L^4 \right] / \mathbb{E}\left[a_L^2 \right] \right) \tag{10}$$

Under the limit, $\sigma_v \to 0$, this result simplifies to the value that appeared in [6], i.e., $R_L^2 = \mathbb{E}\left[a_L^4 \right] / \mathbb{E}\left[a_L^2 \right]$. Finally, assuming $v = 0$, we obtain the value of R_L (for a generic p) in a noise free environment, *viz*

$$R_L^p = \mathbb{E}\left[|a_L|^{p+2} \right] / \mathbb{E}\left[a_L^2 \right]. \tag{11}$$

From (11), for $p = 1$, we obtain $R_L = 2.8, 5.9$ and 11.95 for 16-, 64- and 256-QAM, respectively. For $p = 2$, we obtain $R_L = 2.86, 6.08$ and 12.34 for 16-, 64- and 256-QAM, respectively. Now we express the value of Lagrange multiplier in a noise-free scenario: $\lambda = -0.5(p+2)\mathbb{E}\left[|a_L|^{p+2} \right] / \mathbb{E}\left[a_L^2 \right]$, where the *negative* sign indicates that we need to *maximize* output energy while *minimizing* the higher-order moments.

2.2 Automatic Phase-Recovery Capability

Suppose θ is a residual phase-offset error (in the absence of noise and ISI), it gives $y_n = a_{n'} \exp(\imath\theta)$. Keeping the four-quadrant symmetry of square-QAM in mind, it is desirable that the cost-function of cMMA(p) exhibits local minima at $\theta = 0, \pi/2, \pi$ and $3\pi/2$; similarly, local maxima are required to occur at $\theta = \pi/4, 3\pi/4, 5\pi/4$, and $7\pi/4$. Consider cMMA(2), we can show that

$$J(\theta) = \frac{1}{4} \mathbb{E}\left[a_R^4 + a_I^4 - 6 a_R^2 a_I^2 \right] \cos(4\theta) + \underbrace{\text{constant}}_{\text{w.r.t. } \theta} \tag{12}$$

Note that $\mathbb{E}\left[a_R^4 + a_I^4 - 6a_R^2 a_I^2\right]$ is a sort of kurtosis of square-QAM and it is negative due to the sub-Gaussian nature of QAM signals; consequently, the cost exhibits desired stationary points for $p = 2$. Similar evidence can be found easily for higher values of p.

3. DYNAMIC CONVERGENCE ANALYSIS

We carry out the ODE analysis to gain some understanding in the *dynamic* convergence behavior of the proposed equalizer. In the sequel, we use the notation $[\mathbf{T}]_{ij}$ to denote the element of matrix $\mathbf{T}$ in its ith row and jth column, and $[\mathbf{t}]_i$ to denote the ith element of array $\mathbf{t}$. The covariance matrix of regressor is $\mathbf{R} = \mathbb{E}\left[\mathbf{x}_n \mathbf{x}_n^H\right] = P_a \mathbf{H}\mathbf{H}^H + P_\vartheta \mathbf{I}_N$, where P_a and P_ϑ are respectively the average energies of the signal a_n and additive noise ϑ_n; $\mathbf{I}_N$ is identity matrix of order N and $\mathbf{H}$ is the channel matrix [8]. Exploiting eigen-decomposition, we get $\mathbf{R} = \mathbf{U}^H \mathbf{\Lambda} \mathbf{U}$, where $\mathbf{\Lambda}$ is a diagonal matrix whose diagonal elements are the eigenvalues of $\mathbf{R}$, and $\mathbf{U}$ is an orthonormal matrix. Using $\mathbf{U}$, the transformed update is given as $\widetilde{\mathbf{w}}_{n+1} = \widetilde{\mathbf{w}}_n + \mu \mathbf{\Phi}(y_n)^* \widetilde{\mathbf{x}}_n$, where $\widetilde{\mathbf{w}}_n \equiv \mathbf{U}\mathbf{w}_n$, $\widetilde{\mathbf{x}}_n \equiv \mathbf{U}\mathbf{x}_n$ and $y_n = \widetilde{\mathbf{w}}_n^H \widetilde{\mathbf{x}}_n$. The correlation matrix of $\widetilde{\mathbf{w}}_n$ is

$$[\mathbf{C}_{\widetilde{w}}]_{ij} = \mathbb{E}\left[\widetilde{w}_{n,i} \widetilde{w}_{n,j}^*\right] = \begin{cases} m_{n,i} m_{n,j}^* & i \neq j \\ \Gamma_{n,i} & i = j \end{cases} \tag{13}$$

where $\mathbf{m}_n \equiv \mathbb{E}[\widetilde{\mathbf{w}}_n] = [m_{n,0}, \cdots, m_{n,N-1}]$, $\Gamma_{n,i} \equiv \mathbb{E}\left[|\widetilde{w}_{n,i}|^2\right]$, $(i = 0, \cdots, N-1)$ and $\mathbf{\Gamma}_n = [\Gamma_{n,0}, \cdots, \Gamma_{n,N-1}]$. We obtain

$$m_{n+1,i} = m_{n,i} + \mu \mathbb{E}\left[\mathbf{\Phi}(y_n)^* \widetilde{x}_{n-i}\right] \tag{14}$$

$$\Gamma_{n+1,i} = \Gamma_{n,i} + \mu^2 \mathbb{E}\left[|\mathbf{\Phi}(y_n)|^2 |\widetilde{x}_{n-i}|^2\right] + 2\mu \mathbb{E}\left[\Re\left[\widetilde{w}_{n,i}^* \mathbf{\Phi}(y_n)^* \widetilde{x}_{n-i}\right]\right] \tag{15}$$

Defining $\rho = \mathrm{diag}[\mathbf{\Lambda}]$ and $\eta = \mathbf{U}\mathbf{h}$, we present an approximate expression for the instantaneous residual ISI (deduced from [9, page: 858-9]):

$$\begin{aligned} \mathrm{ISI}_n &\approx \frac{\mathrm{var}(y_n | a_n, \widetilde{\mathbf{w}}_n) - \mathbb{E}\left[\left|\sum_i \vartheta_{n-i} \widetilde{w}_{n,i}^*\right|^2 | \widetilde{\mathbf{w}}_n\right]}{\mathbb{E}[|a_n|^2]} \\ &\approx \frac{\rho^T \mathbf{\Gamma}_n - P_a \eta^H \mathbf{C}_{\widetilde{w}} \eta - P_\vartheta \mathbf{1}^T \mathbf{\Gamma}_n}{P_a |\mathbf{m}_n^H \eta|^2} \end{aligned} \tag{16}$$

where $\mathbf{1}$ is an N-element column-vector of ones. Readers can refer to [10] for detail on recursions (14) and (15) for a *generic* Bussgang BE algorithm.

4. SIMULATION RESULTS

We study the performances in terms of (residual) ISI convergence traces of KDA(p) and cMMA(p) with $p = 1, \cdots, 4$. We consider the transmission of QAM signal over a complex-valued voice-band telephonic channel already considered in [11]. This channel also introduces a phase shift which causes a rotation in signal orientation by 43-44 degree. The input-SNR was taken as 30 and 34 [dB] for 16- and 64-QAM, respectively. A seven-tap equalizer was used with central single-spike initialization. The analytic and simulated ISI traces for 16- and 64-QAM obtained from cMMA(p) are depicted in Fig. 1-4. For KDA(p), we only depict simulation based results. Note that each simulated trace is obtained as an ensemble average of over 200 Monte-Carlo realizations with independent generation of noise and data symbols.

In Fig. 1 and 3, note that the ISI convergence traces obtained from ODE analysis and Monte-Carlo simulations are in full agreement with each other. Secondly note that the ISI mitigation performance of cMMA(p) is far better than that of KDA(p) for both QAM sizes considered in our simulation. In fact we have noticed that the cMMA(p) is capable of giving consistent performance for QAM size as large as 1024. Also note that the cMMA(p) is providing a trade-off between complexity and performance; with a larger p, we are able to get a faster convergence at the cost of more computation.

In Fig. 2 and 4, the eye-opening behavior is illustrated for cMMA(4)/KDA(4) for 16- and 64-QAM, respectively. Observe that the cMMA(4) successfully removed the phase-offset introduced by the channel leading to a clear eye-opening and facilitating a possible switch-over to decision-directed mode. On the other hand, the KDA(4) restored the orientation only for 16-QAM and due to low energy of equalized signal, a reliable switch-over to decision-directed mode can be seen to be not possible (unless a automatic gain control mechanism is employed).

5. CONCLUSIONS

We have proposed a family of memoryless Bussgang-type blind algorithms for joint equalization and carrier phase-recovery of square-QAM signals over complex-valued transmission channel. The main contribution resides in modifying an existing approximation of convex cost-function leading to a new family of algorithms. Analysis of equalizer gain evaluation and dynamic convergence behavior have been described. The convergence analysis is also shown to be in conformation with simulation results.

Acknowledgement: S. Abrar would like to acknowledge the financial support of the Overseas Research Studentship Awards Scheme, UK, the University of Liverpool, UK, and COMSATS Institute of Information Technology (CIIT), Islamabad, Pakistan. He is on leave of absence from the CIIT for higher studies.

REFERENCES

[1] S. Bellini, "Bussgang techniques for blind equalization," *Proc. IEEE GLOBECOM'86*, pp. 1634–1640, Dec. 1986.

[2] Y. Li and Z. Ding, "Convergence analysis of finite length blind adaptive equalizers," *IEEE Trans. Signal Processing*, vol. 43, no. 9, pp. 2120–2129, 1995.

[3] V. Shtrom and H.H. Fan, "New class of zero-forcing cost functions in blind equalization," *IEEE Trans. Signal Processing*, vol. 46, no. 10, pp. 2674, 1998.

[4] R.A. Kennedy and Z. Ding, "Blind adaptive equalizers for quadrature amplitude modulated communication systems based on convex cost functions," *Opt. Eng.*, vol. 31, no. 6, pp. 1189–1199, 1992.

[5] C.R. Johnson, Jr., P. Schniter, T.J. Endres, J.D. Behm, D.R. Brown, and R.A. Casas, "Blind equalization using the constant modulus criterion: A review," *Proc. IEEE*, vol. 86, no. 10, pp. 1927–1950, 1998.

[6] J. Yang, J.-J. Werner, and G.A. Dumont, "The multimodulus blind equalization and its generalized algorithms," *IEEE Jr. Sel. Areas Commun.*, vol. 20, no. 5, pp. 997–1015, 2002.

[7] S. Abrar, A. Zerguine, and M. Deriche, "Soft constraint satisfaction multimodulus blind equalization algorithms," *IEEE Sig. Processing Lett.*, vol. 12, no. 9, pp. 637–640, 2005.

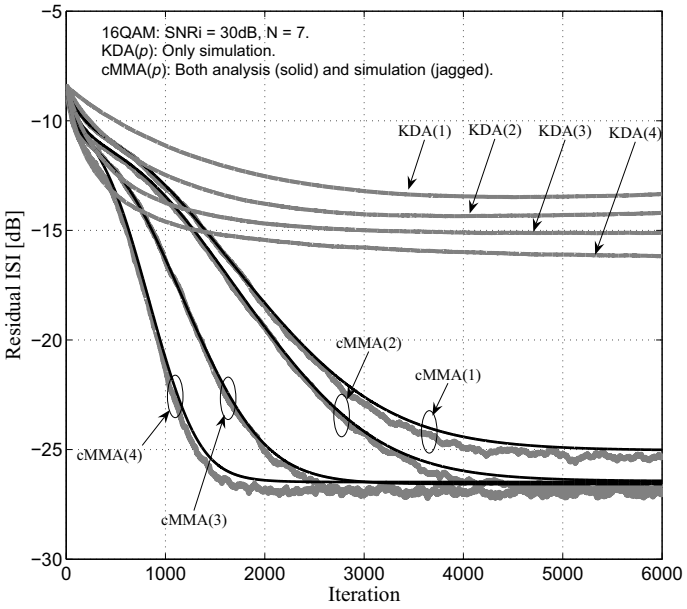

Figure 1: ISI traces for 16-QAM. The $\mu = 2.0 \times 10^{-4}$, 4.0×10^{-5}, 1.5×10^{-5} and 6.0×10^{-6} for cMMA(1), cMMA(2), cMMA(3) and cMMA(4), respectively. The $(\mu_1, \mu_2) = (1 \times 10^{-5}, 3.5 \times 10^{-5}), (6 \times 10^{-6}, 1.2 \times 10^{-6}), (3.2 \times 10^{-6}, 3.8 \times 10^{-6})$ and $(1.5 \times 10^{-6}, 1.5 \times 10^{-6})$ for KDA(1), KDA(2), KDA(3) and KDA(4), respectively.

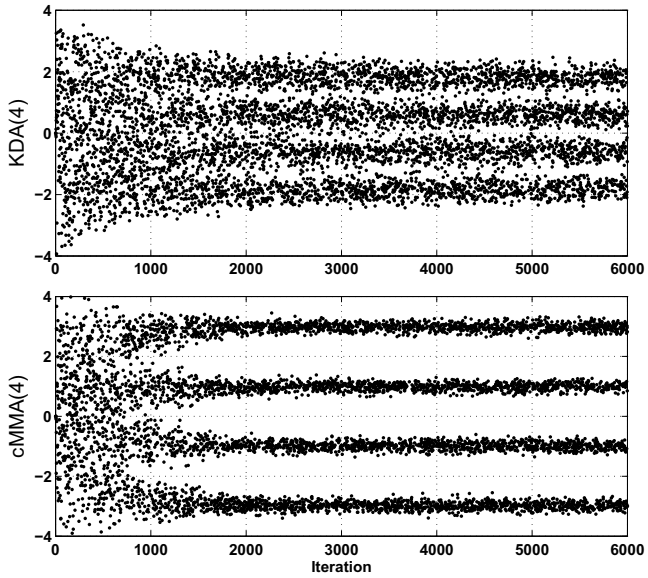

Figure 2: Eye-opening scatter-plot for 16-QAM.

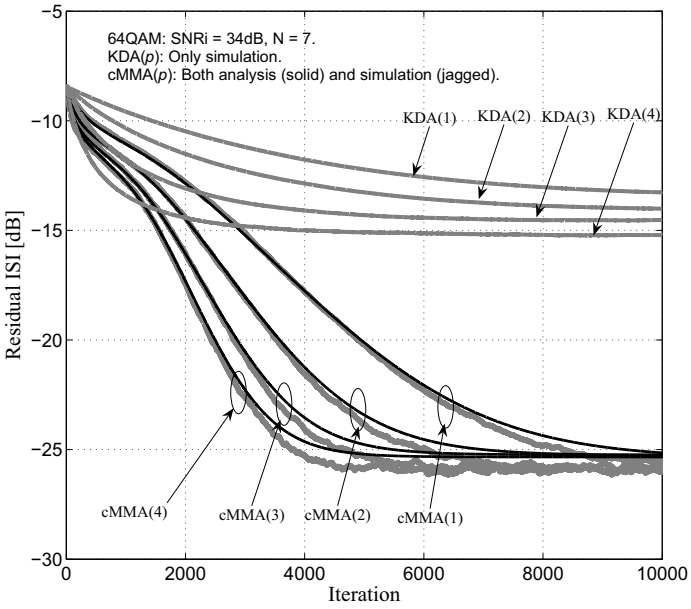

Figure 3: ISI traces for 64-QAM. The $\mu = 1.2 \times 10^{-5}$, 1.44×10^{-6}, 2×10^{-7} and 2.8×10^{-8} for cMMA(1), cMMA(2), cMMA(3) and cMMA(4), respectively. The $(\mu_1, \mu_2) = (4 \times 10^{-7}, 1.4 \times 10^{-6}), (1 \times 10^{-7}, 2 \times 10^{-7}), (3.0 \times 10^{-8}, 3.6 \times 10^{-8})$ and $(1.0 \times 10^{-8}, 1.0 \times 10^{-8})$ for KDA(1), KDA(2), KDA(3) and KDA(4), respectively.

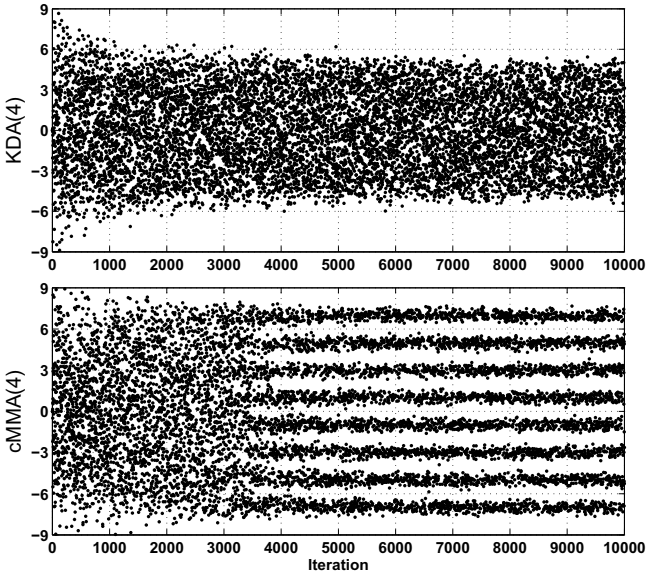

Figure 4: Eye-opening scatter-plot for 64-QAM.

[8] L.M. Garth, "A dynamic convergence analysis of blind equalization algorithms," *IEEE Trans. Commun.*, vol. 49, no. 4, pp. 624–634, 2001.

[9] V. Weerackody, S.A. Kassam, and K.R. Laker. Convergence analysis of an algorithm for blind equalization. *IEEE Trans. Commun.*, 39(6):856–865, 1991.

[10] S. Abrar and A.K. Nandi. Blind Equalization of Square-QAM Signals: A Multimodulus Approach. to appear in *IEEE Transactions on Communications*, vol. 58, no. 6, June 2010.

[11] G. Picchi and G. Prati, "Blind equalization and carrier recovery using a 'stop-and-go' decision-directed algorithm," *IEEE Trans. Commun.*, vol. 35, no. 9, pp. 877–887, 1987.

[12] S. Haykin, *Blind deconvolution*, Prentice Hall, 1994.